Journal of Solid State Chemistry 183 (2010) 198–207

Contents lists available at ScienceDirect

Journal of Solid State Chemistry

journal homepage: www.elsevier.com/locate/jssc

Comparative study of the synthesis of layered transition metal molybdates

S. Mitchell, A. Gómez-Avilés [1], C. Gardner, W. Jones *

Department of Chemistry, The University of Cambridge, Lensfield Road, Cambridge CB2 1EW, UK

ARTICLE INFO

Article history:
Received 11 August 2009
Received in revised form
14 October 2009
Accepted 15 October 2009
Available online 28 October 2009

Keywords:
Layered double hydroxides
Mixed metal oxides
Transition metal molybdates
Calcination and rehydration

ABSTRACT

Mixed metal oxides (MMOs) prepared by the mild thermal decomposition of layered double hydroxides (LDHs) differ in their reactivity on exposure to aqueous molybdate containing solutions. In this study, we investigate the reactivity of some *T*–Al containing MMOs (*T*=Co, Ni, Cu or Zn) towards the formation of layered transition metal molybdates (LTMs) possessing the general formula $AT_2(OH)(MoO_4)_2 \cdot H_2O$, where $A=NH_4^+$, Na^+ or K^+. The phase selectivity of the reaction was studied with respect to the source of molybdate, the ratio of T to Mo and the reaction pH. LTMs were obtained on reaction of Cu–Al and Zn–Al containing MMOs with aqueous solutions of ammonium heptamolybdate. Rehydration of these oxides in the presence of sodium or potassium molybdate yielded a rehydrated LDH phase as the only crystalline product. The LTM products obtained by the rehydration of MMO precursors were compared with LTMs prepared by direct precipitation from the metal salts in order to study the influence of preparative route on their chemical and physical properties. Differences were noted in the composition, morphology and thermal properties of the resulting products.

1. Introduction

Molybdenum containing compounds are important in the field of catalysis as they are known to be catalytically active for several processes including oxidative dehydrogenation (e.g. of simple alkanes [1,2]), hydrodesulfurization (e.g. of petroleum [3]) and selective oxidation (e.g. the epoxidation of alkenes [4] or alkyl olefins [5] or for the selective oxidation of alcohols [6]). The catalytic properties of transition metal molybdates (TMMs) containing first row transition metals have been studied where the transition metal(s) may also play a catalytic role. As transition metals frequently exist in more than one stable oxidation state, transition metal containing compounds often exhibit porosity due to the high structural flexibility of their constituents [7,8]. In addition to their catalytic properties, TMMs also attract attention due to the diverse and potentially tuneable, optical, electronic and magnetic properties which they may possess [9,10].

It is possible to synthesise layered TMMs (LTMs) of general formula $AT_2OH(MoO_4)2(H_2O)$ where $T^{2+}=Mn^{2+}$, Fe^{2+}, Co^{2+}, Ni^{2+}, Cu^{2+} or Zn^{2+} (or a combination of these metals) and $A^+=NH_4^+$, Na^+ or K^+. Layered materials are of particular interest for their intercalation chemistry, large potentially accessible internal surface area and as precursors for the generation of 2D nano-sheets [11]. Table 1 reports the LTMs of this series which, to our knowledge, are known to exist. Two structural polytypes have been identified which were classified by Pezerat as the Φ_x and Φ_y phases, respectively [25]. Simulated structures and PXRD patterns of these phases are shown in Fig. 1. In the Φ_x structure the layers are composed of chains of edge sharing transition metal octahedra which are connected by tetrahedral molybdate groups [24]. In the Φ_y structure transition metal octahedra edge share to form sheets. In this case, the molybdate tetrahedra cap an ordered cation vacancy [19]. The layers stack in the c direction and are held together by electrostatic and hydrogen bonding interactions. The layers are negatively charged, electroneutrality being maintained by the incorporation of charge balancing cations (A^+) within the interlayer space. Whereas the Φ_x structure has been obtained with $A^+=Na^+$, K^+ or NH_4^+, the Φ_y polytype has to date only been reported for $A^+=NH_4^+$.

The synthesis of LTMs has not been widely studied. Many of the LTMs reported to date were isolated by authors investigating the reaction between different transition metal salts with alkali molybdate species. In general their synthesis was not specifically targeted but rather the intention was to prepare novel mixed metal materials with potentially interesting (catalytically active, porous, etc.) properties [15]. An alternative synthetic route for the preparation of LTMs of the Φ_y structure which involved the rehydration of a mixed metal oxide (MMO), derived from a *T*–Al layered double hydroxide (LDH) [26,27] precursor, in an aqueous ammonium heptamolybdate solution was introduced by Levin et al. [23]. LTMs were successfully obtained with $T^{2+}=Zn^{2+}$ or a mixture of Zn^{2+} and Cu^{2+} or with Co^{2+} or Ni^{2+} but not with Mg^{2+}

* Corresponding author. Fax: +44 1223 336017.
E-mail address: wj10@cam.ac.uk (W. Jones).
[1] Visiting from: Instituto de Ciencia de Materiales, CSIC, Cantoblanco 28049, Madrid, Spain.

0022-4596/$ - see front matter Crown Copyright © 2009 Published by Elsevier Inc. All rights reserved.
doi:10.1016/j.jssc.2009.10.011

or Ni^{2+} as the only divalent metal. This method provides an alternative, low temperature, environmentally friendly (e.g. due to the elimination of NO_3^- waste streams) preparation route.

In this study, we report the reaction of *T*–Al MMOs where *T*=Co, Ni, Cu or Zn with aqueous solutions containing ammonium heptamolybdate or sodium or potassium molybdate. The extent of molybdate polymerisation in aqueous solution (MoO_4^{2-}, $Mo_7O_{24}^{6-}$, etc.) is known to be influenced by both the solution pH and concentration of molybdate species present [28]. The solution pH also influences the extent of LDH dissolution [29]. For these reasons we have investigated the influence of reaction conditions including the ratio of *T* to Mo, reaction pH and the LDH precursor crystallite size on the reactivity of the MMOs. We compare the LTM products prepared by the rehydration method with analogous LTMs synthesised via the standard route of precipitation in terms of their composition, morphology and thermal properties. As the properties of MMOs derived from layered precursors may be influenced by the preparative route of the layered precursor [30], we also study the influence of precursor preparation route on the LTMs obtained.

Table 1
Summary of T^{2+} and A^+ combinations and observed structure of LTMs previously reported of general formula $AT_2OH(MoO_4)_2 \cdot H_2O$.

T^{2+}	A^+		
	NH_4^+	Na^+	K^+
Mn^{2+}	Φ_x [12]	Φ_x [13]	Φ_x [14]
Fe^{2+}	–	Φ_x [15]	Φ_x [16]
Co^{2+}	Φ_x[a] [17]	Φ_x [17,18]	Φ_x [17]
Ni^{2+}	Φ_y [19]	Φ_x [20,21]	Φ_x [17]
Cu^{2+}	Φ_y [22]	–	–
Zn^{2+}	Φ_y [21,23]	Φ_x [17,24]	Φ_x [17]

[a] Reported by Pezerat et al. to have the Φ_x structure. We have synthesised this compound with the Φ_y structure.

2. Experimental section

2.1. Chemicals

All chemicals used were reagent grade, used as supplied by Sigma–Aldrich.

2.2. MMO method

Precursor LDHs were prepared both by the commonly reported route of coprecipitation [26,27] and by the urea hydrolysis method, a method which is known to yield LDH products with a higher aspect ratio [31]. In the coprecipitation synthesis, a 50 ml mixed metal salt solution containing $T(NO_3)_2 \cdot xH_2O$ (0.02 mol), where T^{2+}=Zn^{2+}, Cu^{2+}, Ni^{2+} or Co^{2+}, and $Al(NO_3)_3 \cdot 9H_2O$ (0.01 mol) and an aqueous solution containing NaOH (2 M) and Na_2CO_3 (2 M) were prepared. These solutions were combined by dropwise additions to distilled water (50 ml) heated at 55 °C, at relative rates such that a constant pH of 9.0 ± 0.1 was maintained. Following precipitation the solution was then aged for 24 h at 70 °C. The resulting precipitates were collected by filtration, washed and dried. For the urea hydrolysis method, a 50 ml metal salts and urea solution was prepared by dissolving $Zn(NO_3)_2 \cdot 6H_2O$ (0.666 mol) with $Al(NO_3)_2 \cdot 9H_2O$ (0.333 mol)

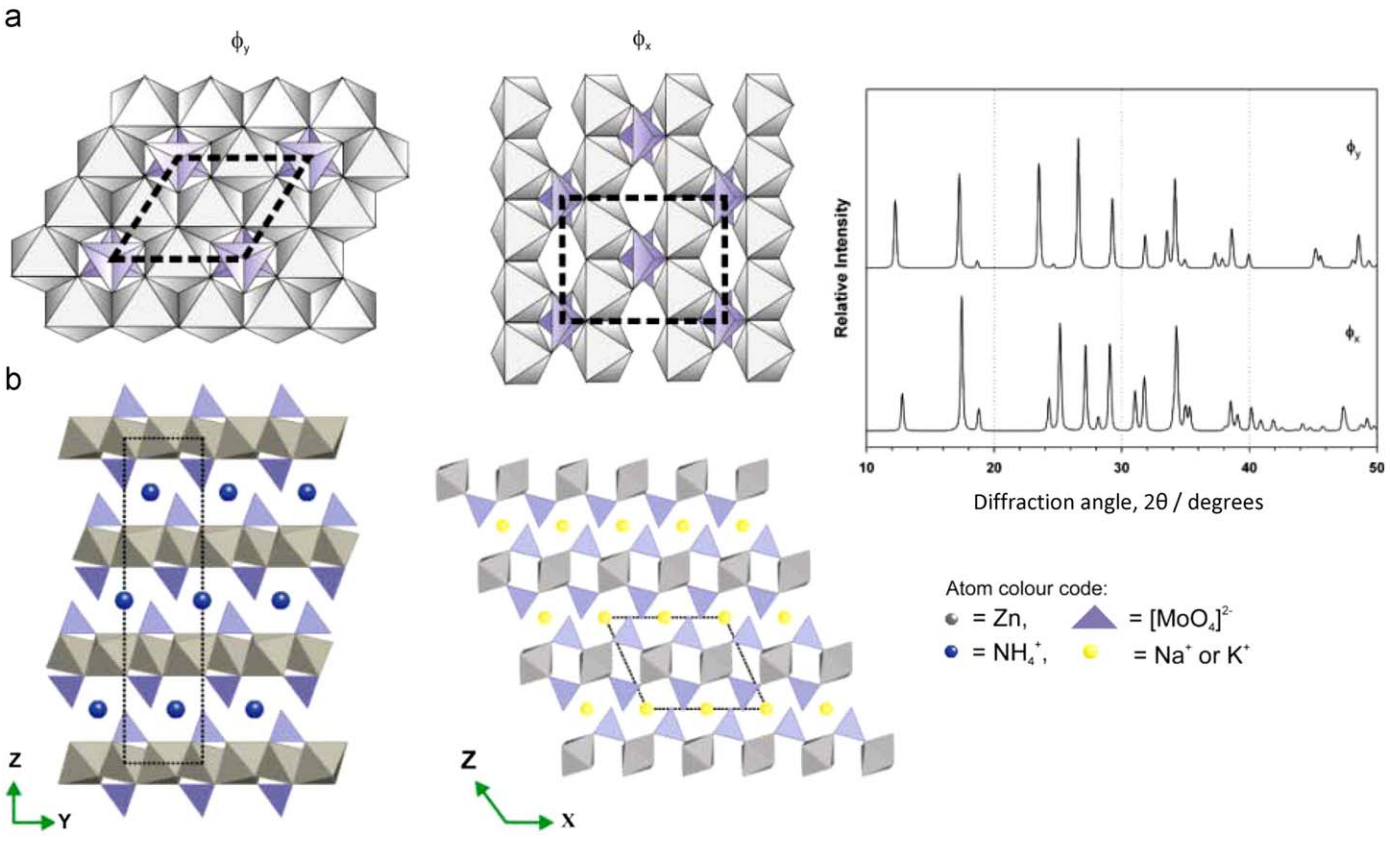

Fig. 1. Schematic diagram of (a) the Φ_y and (b) the Φ_x LTM structures of general formula $AT_2OH(MoO_4)_2 \cdot H_2O$, projected along the (110) plane. The simulated PXRD patterns for these structures (c) are also shown.

and urea such that $[T^{2+}]+[Al^{3+}]=1\,mol\,dm^{-3}$ and [urea]/$([T^{2+}]+[Al^{3+}])=3.3$ in distilled water. The solution was then heated at 110 °C under reflux for 24 h. The resulting precipitate was collected, washed and dried.

Formation of MMOs was achieved by calcination of the precursor LDHs in a carbolite furnace at 500 °C for 3.5 h. Calcination temperatures of 350, 250 and 200 °C were also used when the MMO obtained at 500 °C was found to be unreactive during the rehydration step.

A typical procedure to study MMO reactivity involved reacting the MMO (0.25 g) with a 50 ml solution of ammonium heptamolybdate or sodium or potassium molybdate ([*T*]/[Mo]) prepared with distilled water. The mixture was stirred for 4 h and the resulting product collected by filtration, washed and dried. The influence of the *T*/Mo ratio was studied for MMOs which were found to be reactive towards the formation of LTMs. Reactions were undertaken with varying concentrations of ammonium heptamolybdate solutions (0.2, 0.1, 0.05 and 0.025 M). Similarly the influence of pH was studied by adjusting the pH after addition of the MMO precursor to the molybdate solution by addition of aqueous solutions of NH_4OH (35%)/NaOH (1 M) and HNO_3 (1 M) depending on the source of molybdate used.

2.3. Precipitation method

Here, LTMs were isolated on reaction of MMOs ($T^{2+}=Zn^{2+}$, Cu^{2+} and $A^{+}=NH_4^{+}$), analogous LTMs were prepared by solution precipitation from the metal salts. It should be noted that LTM phases may be isolated from solution under a wide range of conditions, the specific conditions indicated were those used to obtain the LTMs synthesised for comparative purposes in this work. Aqueous solutions containing the desired transition metal nitrate (0.007 mol) and $(NH_4)_6Mo_7O_{24}\cdot 4H_2O$ (0.001 mol) were prepared using distilled water (50 ml) with a *T*/Mo ratio of 1. LTM precipitation was induced by increasing the pH to approximately 6 (for *T*=Cu) or pH 8 (for *T*=Zn) by the addition of a basic solution of NH_4OH (35%). The resulting solutions were then aged at 60 °C for 4 h. After ageing the precipitates were collected by filtration, washed with distilled water and oven dried at 100 °C.

2.4. Experimental techniques

Powder X-ray diffraction (PXRD) patterns of the resultant materials were recorded using a Philips PW3710 diffractometer in reflection geometry using graphite monochromated Cu*K*α radiation. Data were collected from finely ground samples pressed on a flat plate, glass sample holder. Phase identification was achieved by comparison with PXRD patterns simulated, using the X'Pert Plus software, from single crystal structural information data; $NaZn_2OH(MoO_4)_2(H_2O)$ (Φ_x structure) no. 305, $H_3NH_4Zn_2Mo_2O_{10}$ (Φ_y structure) no. 24967, as reported in the International Crystal Structure Database. Variable temperature data were collected using an Anton Parr TTK450 low temperature attachment. The sample was heated, at a heating rate of 10 °C min^{-1}, to the desired temperature and held at that temperature while the data were collected. Measurements were performed every 25 °C increment from 25 to 450 °C.

Fourier Transform Infra-Red (FTIR) spectra were recorded on a ThermoNicolet Nexus Spectrometer using the Smart Golden Gate Single Reflection stage Attenuated Total Reflection. A background spectrum was recorded before the sample was placed on the sample stage, pressure applied using a sapphire anvil, and data acquired. Data were recorded in the range $\nu=550$–$4000\,cm^{-1}$.

Thermal analysis was performed on a Mettler Toledo SDTA 851 thermal balance. Thermal gravimetric (TG) and differential thermal gravimetric (DTG) curves were obtained by heating the sample (10–20 mg) from 25 to 800 °C in air, at a ramp rate of 10 °C min^{-1}. In cases where evidence of sample oxidation was observed (i.e. for samples containing *T*=Cu) the measurements were repeated under a flow of N_2 gas (30 ml min^{-1}).

Scanning electron microscopy (SEM) was undertaken using a JEOL 5800LV instrument. Samples were dispersed from ethanol onto a freshly cleaved Mica surface. A thin platinum coating was applied to reduce the effects of sample charging.

Compositional analysis of C, H and N content was carried our by the Microanalysis Service at the Department of Chemistry, University of Cambridge. The *T*/Mo ratio was also analysed by energy dispersive X-ray diffraction (EDX) using the JEOL 5800 LV instrument with an accelerating voltage of 30 KeV. The samples used for these measurements were not coated with Pt. Results were averaged over a minimum of 5 sites per sample. Analysis of the accuracy of the EDX was undertaken by calibration with samples of known composition. The *T*/Mo ratio obtained for a $ZnMoO_4$ sample (Sigma–Aldrich), for example, was found to be 1.0/1.1 with a standard deviation of ± 0.12.

3. Results and discussion

3.1. Nomenclature

Samples prepared during this study are described by the following nomenclature:

T_C_M
T is the transition metal studied **Zn**, **Cu**, **Ni** or **Co**.
C indicates the nature of the compound: **LDH**, **MMO** or **LTM**.
M indicates the synthesis method: **P** for precipitation, **U** for urea hydrolysis and **MP** or **MU** for synthesis by reaction of a MMO derived from a precursor LDH prepared by coprecipitation (MP) or by urea hydrolysis (MU).

3.2. Reaction of MMO: reactivity

Calcination of precursor LDHs at 500 °C led to decomposition of the layered structure and the formation of a disordered MMO phase, as expected [23]. PXRD patterns of the resultant MMOs show broad,

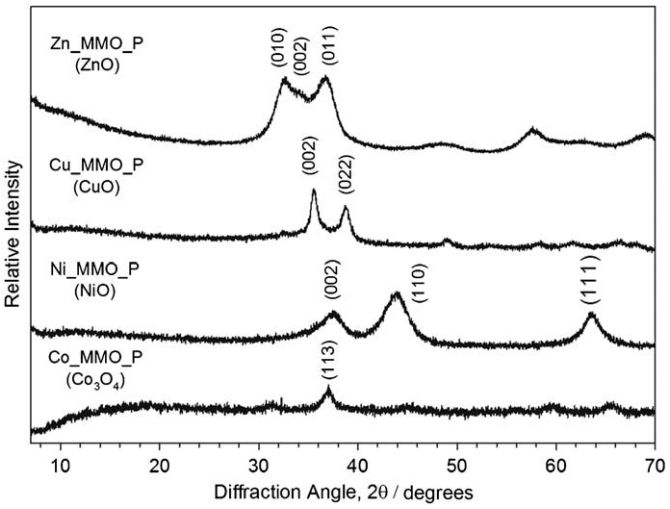

Fig. 2. PXRD patterns of the MMO phases obtained on calcination of their respective precursor LDHs.

Table 2
Crystalline phases identified in the T_MMO_P phases obtained following calcination of T_LDH_P precursors to 500 °C, and in the products resulting from their reaction with aqueous ammonium (NH_4^+) heptamolybdate or sodium (Na^+) or potassium (K^+) molybdate (T: Mo ≈ 1, room temperature).

Precursor	Crystalline phases identified			
	In MMOs	On reaction (NH_4^+)	On reaction (Na^+)	On reaction (K^+)
Co_MMO_P	Co_3O_4	Co_3O_4	Co_3O_4	Co_3O_4
Ni_MMO_P	NiO	NiO	NiO	NiO
Cu_MMO_P	CuO	Φ_y LTM	(CO_3^{2-}) LDH	(CO_3^{2-})LDH
Zn_MMO_P	ZnO	Φ_y LTM	(CO_3^{2-}) LDH	(CO_3^{2-}) LDH

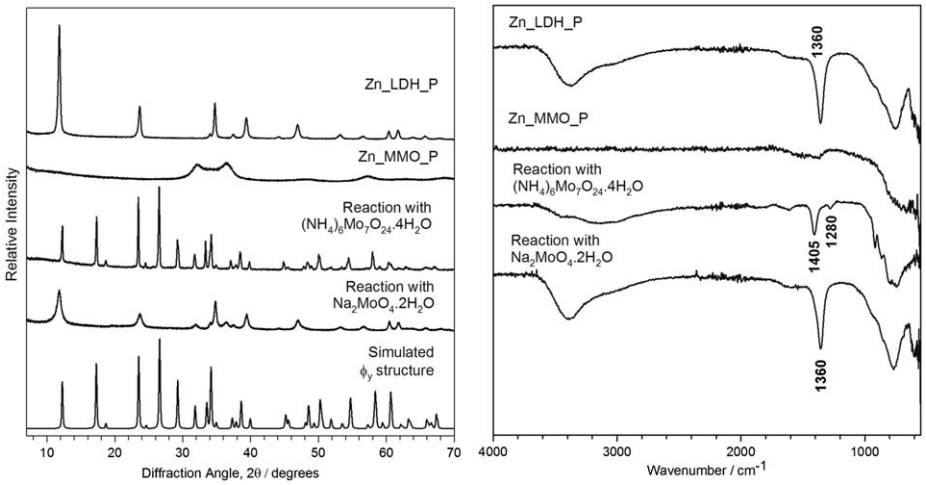

Fig. 3. PXRD and FTIR data of the LDH, MMO precursors and the product obtained on reaction with ammonium heptamolybdate and sodium molybdate solutions for T=Zn^{2+}.

low intensity reflections, in positions corresponding to those reported for oxides of the transition metal (T) studied (Fig. 2). Reflections are indexed according to the crystalline phases identified in Table 2. The location of the Al^{3+} remains the subject of debate. Following mild thermal treatment the aluminium is not thought to phase separate significantly. A higher calcination temperature would be required to detect the formation of a crystalline aluminium containing phase e.g. a spinel or oxide phase [32].

The crystalline phases identified in the materials obtained following attempted reaction of precursor MMOs with ammonium heptamolybdate or sodium or potassium molybdate solutions are also summarised in Table 2. Co and Ni containing MMOs showed little evidence of reactivity under any of the conditions studied. PXRD patterns of the materials collected on reaction of the MMOs remained unchanged from those of the precursor MMOs. The use of lower calcination temperatures during MMO preparation was not found to improve their reactivity. Zn and Cu containing MMOs, in contrast, were reactive in all attempted reactions. Fig. 3 shows the PXRD and FTIR analysis of the precursor and product phases obtained for Zn. Corresponding data for Cu may be found in the supplementary material. Reaction of the MMOs in the presence of ammonium heptamolybdate solutions yielded single phase Φ_y LTM products. Changing the source of molybdate to sodium or potassium molybdate led to a change in the phase selectivity with reflections corresponding to a reconstructed LDH phase appearing in the PXRD patterns. FTIR analysis of the reconstructed LDH phases shows the reappearance of a strong band at 1360 cm^{-1} indicating the presence of CO_3^{2-}. Based on the ideal compositions where a T/Mo ratio of 4 or 1.7 would be expected for $(MoO_4)^{2-}$ or $(Mo_7O_{24})^{6-}$ containing LDHs for a Zn/Al ratio of 2, respectively, the EDX analysis confirmed that molybdate was not incorporated significantly in these products (Zn/Mo=22 or Cu/Mo=18).

3.3. Reaction of MMO: influence of T/Mo ratio

The formation of LTMs of Φ_y structure on reaction of Zn_MMO_P or Cu_MMO_P precursors with ammonium heptamolybdate was found to be highly dependent on the T/Mo ratio in solution. PXRD patterns of the materials obtained on reaction of Zn_MMO_P at molybdate concentrations of between 0.2 and 0.025 M are shown in Fig. 4 (corresponding data for Cu may be found in the supplementary material). The optimal concentration for LTM formation was found to be 0.05 M for both Zn and Cu. Assuming an LDH precursor composition of ideal formula $T_4Al_2(OH)_{12}CO_3 \cdot 2H_2O$ this would correspond to a T/Mo molar ratio of 1. As the concentration of ammonium heptamolybdate was increased a change in the phase selectivity of the reaction was observed. New reflections appeared in the diffraction patterns and those corresponding to the LTM phase decreased in intensity. The sharp, low angle reflection at 2θ=8.2° was particularly noticeable. A search of the ICSD revealed that this new phase bears a close resemblance (Fig. 4) to the family of heteropolyoxomolybdates with the Anderson type structure comprising the $(H_6TMo_6O_{24})^{4-}$ anion (where T=Zn or Cu), NH_4^+ cation and H_2O [33].

3.4. Reaction of MMO: influence of LDH precursor synthesis method

Fig. 5 compares SEM images taken of the LDH and MMO precursors and the LTM products obtained during syntheses with

Zn and Cu. Precursor LDHs prepared by coprecipitation exhibit the features typically reported for this method; a wide particle size distribution with aggregated particles which consist of small (typically < 500 nm), plate-like primary crystallites [34]. Synthesis by the urea hydrolysis method yielded larger (average particle size 2–3 μm), plate-like crystallites, as expected [31]. No significant morphological changes were noted on thermal decomposition of these LDHs to form their corresponding MMOs. The corresponding LTMs formed on reaction of these MMOs are found to have a similar average particle size to those of their precursor LDHs although the LTM products appear morphologically more well-defined. The LDH precursor crystallite size clearly influences that of the LTM product, with the LTM crystallites prepared from LDH precursor Zn_LDH_U significantly larger than those in the LTM prepared from Zn_LDH_P.

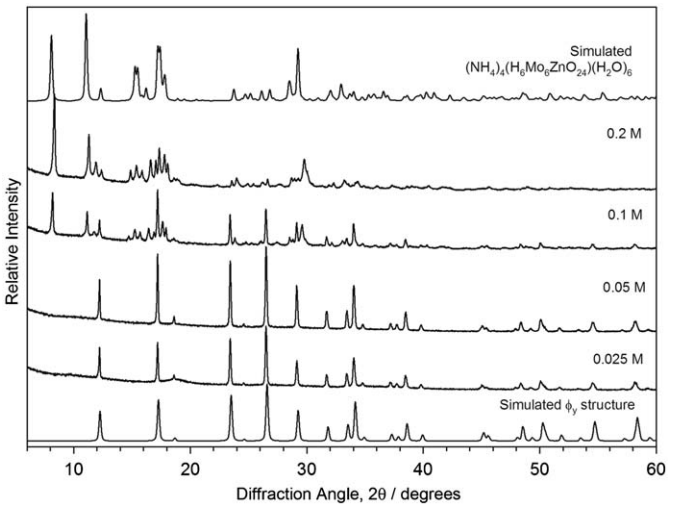

Fig. 4. PXRD analysis of the influence of molybdate concentration of the reaction of Zn_MMO_P.

3.5. Reaction of MMO: influence of pH

The influence of pH on the reactivity of Zn–Al MMOs with ammonium heptamolybdate and sodium molybdate solutions (0.05 M) is shown in Fig. 6. Addition of Zn_MMO_P to a solution of ammonium heptamolybdate (Fig. 6(a)) resulted in an initial pH of 5.4 and in the formation of a single phase Φ_y LTM. Variation of the initial pH between pH 5 and 10 had no significant influence on the reactivity or selectivity of reaction. Reaction with sodium molybdate solution (Fig. 6(b)) gave an initial pH of 9.0 and resulted in the formation of a reconstructed LDH phase. Decreasing the pH to pH 5 led to a change in the phase selectivity of the reaction. At this pH an LTM with the Φ_x structure was collected from solution.

3.6. LTMs: influence of preparative route

LTMs derived from MMO precursors, appear isostructural to those prepared via solution precipitation. No significant differences in the number, position or relative intensities of reflections are observed between the PXRD patterns (Fig. 7) or FTIR spectra of the products obtained. An SEM comparison (Fig. 8) reveals some differences in the microstructures of the LTM products. Crystallites derived from MMO precursors are larger and more uniform than those obtained by precipitation. The particles sizes observed in the products derived from MMO precursors also appear to be influenced by the particle size of the LDH precursor, with larger average particle sizes observed in Zn_LTM_MU products than in Zn_LTM_MP products. An estimate of the crystallite sizes, *s*, of the LTM phases obtained was calculated for comparison using a Scherrer based analysis on the low angle (001) reflection. The results, which are summarised in Table 3, support the observation of the formation

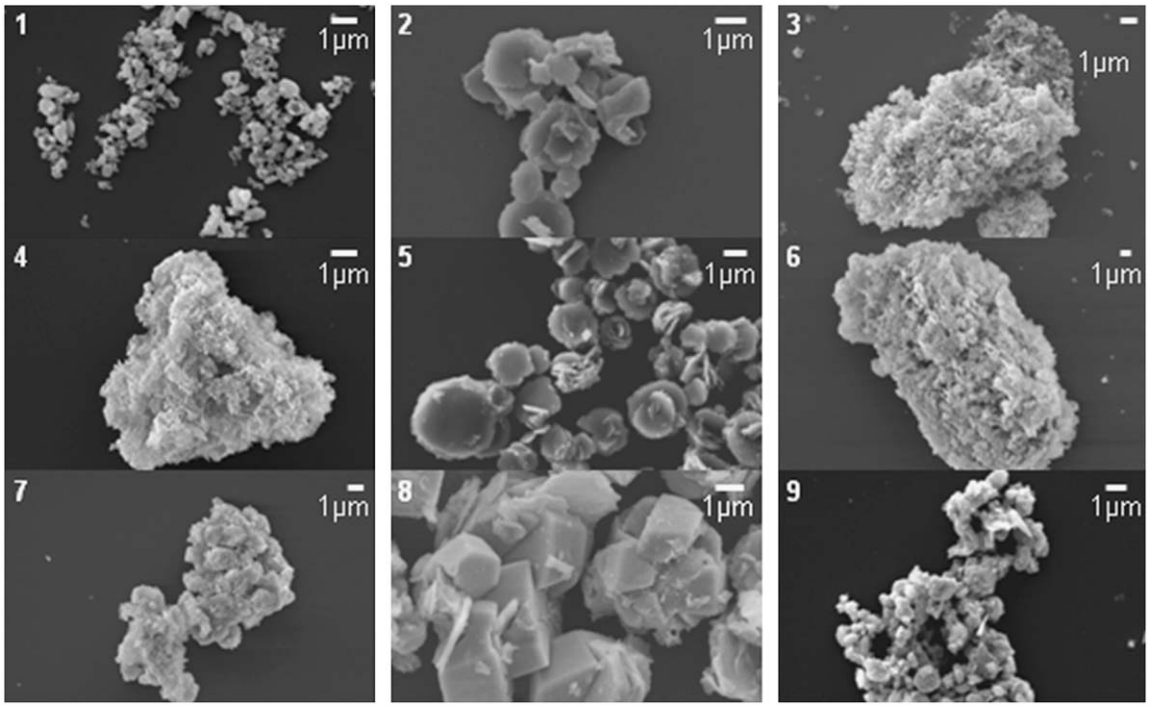

Fig. 5. SEM comparison of: LDH precursors (1) Zn_LDH_P, (2) Zn_LDH_U, (3) Cu_LDH_P; MMO intermediates (4) Zn_MMO_P, (5) Zn_MMO_U, (6) Cu_MMO_P; and LTM products (7) Zn_LTM_MP, (8) Zn_LTM_MU and (9) Cu_LTM_MP.

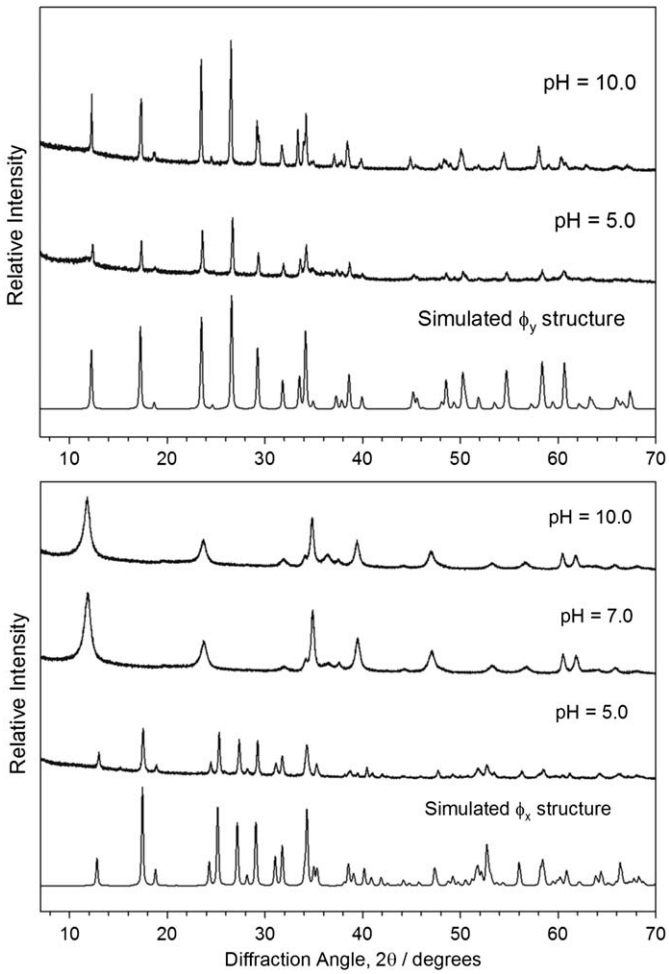

Fig. 6. PXRD analysis of the influence of pH on the reaction of Zn_MMO_P with aqueous ammonium heptamolybdate (top) or sodium molybdate (bottom).

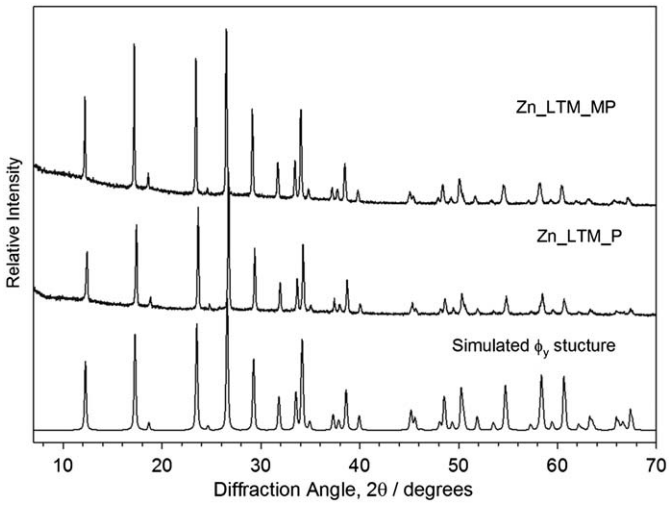

Fig. 7. PXRD comparison of Zn_LTM_MP and Zn_LTM_P compared with the simulated pattern of the Φ_y structure.

of larger crystallites in LTM phases prepared via the MMO route (s=804 nm for Zn_LTM_MP compared with s=492 nm for Zn_LTM_P).

Results of compositional analysis of the precursor and product phases are reported in Table 4. The precursor LDH and MMO phases were found to have T/Al ratios between 1.6 and 1.9 which is slightly lower than the stoichiometry of 2 present in solution during LDH synthesis. As noted by Levin and co-workers for T=Zn the T/Al ratio increased following reaction of the MMO with ammonium heptamolybdate solution [23]. Noticeably the LTM products, however, still contain significant amounts of Al. Maximum loss of Al was observed on reaction of the LDH precursor prepared by urea hydrolysis. The Al content of Cu_LTM_MP obtained on reaction of Cu_MMO_P is comparable to that of the MMO.

3.7. LTMs: characterisation of thermal properties

The TG profiles of Zn and Cu containing LTMs obtained by the two different preparation routes and the PXRD patterns of the residues remaining following their thermal analysis are shown in Fig. 9. As Cu containing samples were found to be sensitive to oxidation during thermal analysis (observed by a weight gain upon heating in air, TG profiles shown in supplementary material), the data presented were recorded under a N_2 gas flow.

On heating the LTM, samples show a gradual weight loss at temperatures below 200 °C. Above this temperature, all samples undergo a sharp weight loss between 200 and 400 °C which can be clearly identified in the corresponding DTG curves (see supplementary material) and is thought to correspond to the simultaneous loss of NH_3 and H_2O from the structure. A further weight loss step, which is more noticeable for the Cu containing samples, is observed above 700 °C. This loss is thought to be due to the sublimation of MoO_3 from the MMO phase which has been previously observed during the thermal decomposition of other Cu containing LTMs [22].

Analysis by FTIR and PXRD of the residues obtained following thermal treatment combined with an *in situ* PXRD study provided further insight into the nature of the LTM decomposition. Bands arising from the NH_4^+ cations (e.g. the characteristic H–N–H bending mode at 1410 cm^{-1}) present in the FTIR spectra of the as synthesised LTMs, remain visible in the residues obtained after heating to 200 °C but are absent in the residues obtained following heat treatment to 400 °C indicating loss of NH_3 from the structure. The *in situ* PXRD study confirmed the disappearance of reflections corresponding to the LTM phase by 400 °C indicating the simultaneous collapse of the LTM structure within this temperature range (Fig. 10). The extrinsic reflections observed in the two theta range of 40–45° are instrumental reflections which arise as a result of diffraction from the high temperature stage used.

Table 5 summarises the temperatures at which the principal weight loss is observed, T_p, the total mass losses measured following heat treatment to 400 °C, TML_{400} and the crystalline phases identified following heat treatment to 800 °C. Ammonium copper molybdate appears to be slightly more stable than ammonium zinc molybdate (T_p=289 or 264 °C for T=Cu or Zn, respectively). The TML_{400} values measured are in general slightly higher than the expected 10.5% mass loss for an LTM of ideal composition [12]. This is thought to be due to the presence of physisorbed water in the as synthesised samples.

Although the form of the TG profiles is similar for LTM products prepared by precipitation compared with those of LTMs synthesised from MMO precursors, some differences may be noted. As the temperature is increased, the LTM products derived from MMOs show a larger initial weight loss (below 200 °C). This weight loss is thought to be related to the loss of physisorbed water from the sample and the differences observed might be a consequence of the differences in sample morphologies between the two samples (Fig. 8). Both products, Zn_LTM_MP and

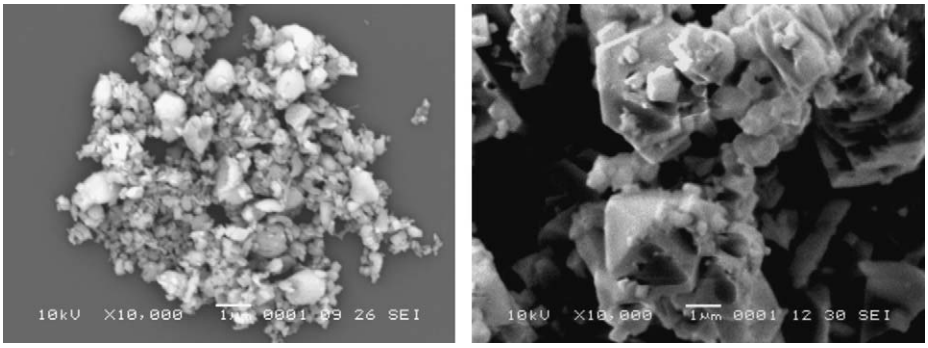

Fig. 8. SEM comparison of LTM products Zn_LTM_P (left) and Zn_LTM_MP (right).

Table 3
Summary of the estimated crystallite sizes, *s*, of the LTM phases obtained, calculated using a Scherrer based analysis for the (001) reflection with a shape factor, k=0.9.

Sample	*s* (nm)
Zn_LTM_P	492
Zn_LTM_MP	804
Zn_LTM_MU	936
Cu_LTM_P	230
Cu_LTM_MP	455

Table 4
Summary of compositional analyses of the LDH, MMO and LTM phases obtained during synthesis by reaction of MMO precursor.

Sample	Wt% C	Wt% N	T:Mo	T:Al
Zn_LTM_P	0.0	4.9	0.9	–
Zn_LDH_P	1.9	0.0	–	1.7
Zn_MMO_P	0.7	0.0	–	1.8
Zn_LTM_MP	0.0	2.3	1.3	2.5
Zn_LDH_U	2.2	0.0	–	1.6
Zn_MMO_U	0.1	0.0	–	1.9
Zn_LTM_MU	0.1	2.4	1.1	4.0
Cu_LTM_P	0.1	2.6	0.7	–
Cu_LDH_P	2.5	0.0	–	1.6
Cu_MMO_P	1.3	0.0	–	1.9
Cu_LTM_MP	0.1	2.6	1.4	2.2

Cu_LTM_MP, also exhibit a higher stability (based on the measured T_p values) than their counterparts prepared by precipitation (Table 5).

The preparation method of the precursor is also found to influence the stability of the resulting MMOs. MMOs derived from T_LTM_MP precursors exhibit greater weight losses above 700 °C, associated with increased sublimation of MoO_3 from their structures, compared with those observed for MMOs derived from T_LTM_P precursors. Analysis of the residues collected following thermal treatment confirms differences in the nature of the MMO derived from the precursor LTMs dependent on the precursor preparation method (Table 5). Crystalline transition metal oxides of $TMoO_4$ and/or $T_3Mo_2O_9$ structures were observed to form following LTM decomposition depending on the precursor LTM studied.

4. Discussion

The ability of MMO phases, produced by the mild thermal decomposition of LDHs, to reconstruct in aqueous solution has received continued interest. This property is exploited for the decontamination of waste water streams [35,36], the preparation of activated base catalysts [37,38], and for the synthesis of LDHs containing various anionic species which may be difficult to incorporate via other synthetic routes [39,40]. It is thought that, depending on the extent of thermal decomposition and the original LDH composition, the layer structure in the resulting LDH phases remains largely unaltered from that of the precursor [26]. This permits manipulation of the interlayer species without major variation of the stoichiometry or dispersion of the layer metal cations.

By comparison exposure of MMOs to aqueous molybdate containing solutions may result in several eventualities. It is commonly associated with the preparation of (poly)oxomolybdate pillared LDH phases [41] in attempts to prepare novel catalysts with improved properties [42–44]. Layered materials have the potential to serve as a support for the catalytically active species, the supported products acting as environmentally friendly catalysts which can be conveniently recovered and recycled [45] and may show increased catalytic activity and selectivity compared with those of the unsupported catalysts [46]. LTMs have also been studied with a view to their use in similar areas of catalysis as those of molybdate pillared LDHs e.g. for the dehydrogenation of propane [47].

As the rehydration of MMOs in aqueous solution offers an alternative, potentially greener, preparation route for the synthesis of both LTMs and molybdate containing LDHs it is important to understand the distinctive phase selectivity which may result. Fig. 11 summarises the possible outcomes both previously reported and which have been observed during our investigations. The route taken is dependent on several factors including the MMO composition, molybdate source and reaction conditions.

MMOs containing Ni or Co showed little evidence of reactivity under the conditions studied. Ni and Co containing LDHs are known to be difficult to reconstruct following thermal decomposition. For Ni, reversibility is achievable if rehydration is undertaken hydrothermally [48,49]. It was of interest to investigate the influence of the presence of molybdate on the hydrothermal reaction of Ni containing MMOs. Fig. 12 shows the PXRD patterns of the materials obtained following hydrothermal reaction of Ni_MMO_P in the presence of ammonium, sodium and potassium molybdate at 180 °C for 24 h. Changes in the diffraction pattern were observed in all cases with broad, low intensity reflections appearing in positions typical of those expected for an LDH phase. No evidence of LTM formation was observed under these conditions. Where Co is present reconstruction may be possible if the formation of Co_3O_4 spinel is avoided during thermal decomposition by, for example, calcining in a non-oxidising atmosphere [50]. With the desire to

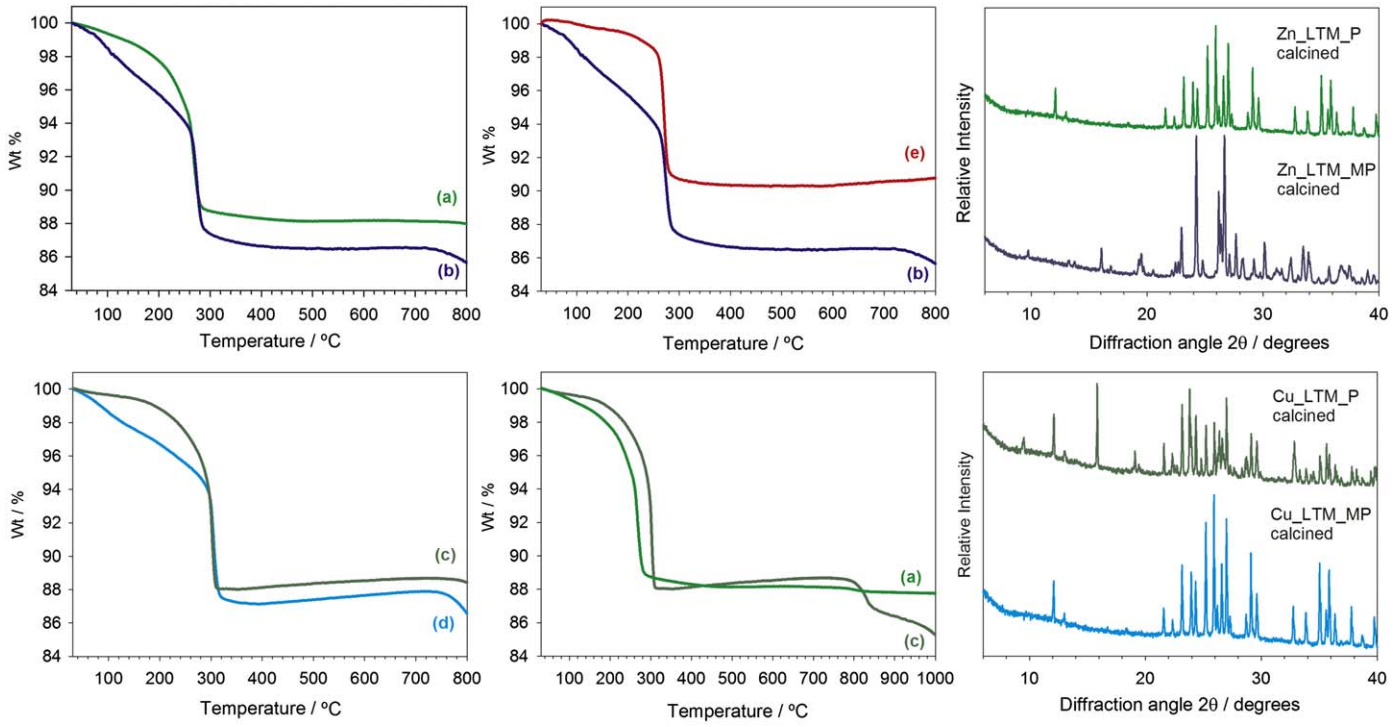

Fig. 9. Comparison of the TG profiles of (a) Zn_LTM_P, (b) Zn_LTM_MP, (c) Cu_LTM_P, (d) Cu_LTM_MP and (e) Zn_LTM_MU recorded under a N_2 gas flow of 30 ml min^{-1}. The PXRD patterns of the residues remaining after their calcination to 800 °C are also shown.

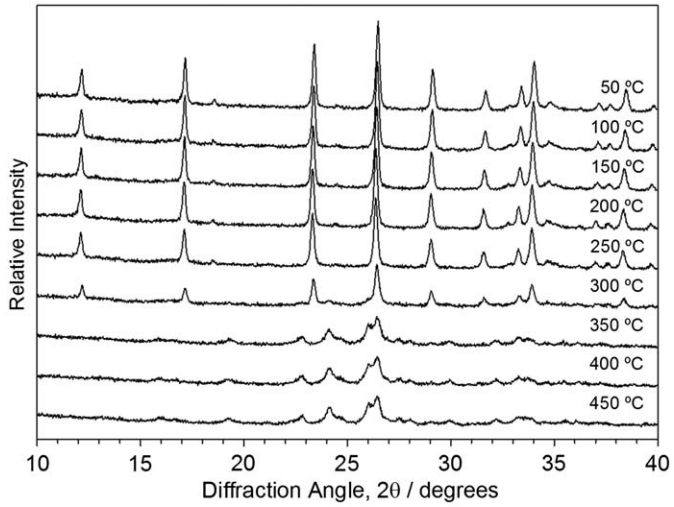

Fig. 10. *In situ* PXRD analysis of the thermal decomposition of Zn_LTM_MP.

Table 5
Summary of the total mass loss at 400 °C, TML_{400}s, temperatures at which the principal weight loss occurs during decomposition, T_ps, and the crystalline phases, CPs, identified in resulting residues for the LTM products obtained.

Sample	T_p (°C)	TML_{400} (%)	CPs
Zn_LTM_P	251	11.7	$Mo_2O_9Zn_3$
Zn_LTM_MP	270	12.0	$ZnMoO_4$
Zn_LTM_MU	275	9.5	$ZnMoO_4$
Cu_LTM_P	289	11.0	$CuMoO_4$
Cu_LTM_MP	305	11.5	$CuMoO_4$ and $Cu_3Mo_2O_9$

promote reactivity of Co_MMO_P precursors, Co containing LDHs were calcined at 350 °C under a N_2 environment for 1 h and the resulting MMOs were reacted with molybdate containing solutions at room temperature and at 100 °C for 24 h. No reaction was observed under any of the conditions studied.

Cu and Zn containing MMOs were reactive under all conditions studied. The phase selectivity of the reaction was found to be dependent on both the source and concentration of molybdate species and on the reaction pH. Formation of LTMs possessing the Φ_y structure was achieved in the presence of NH_4^+ with a *T*/Mo ratio in solution ≈ 1. This structure has only previously been reported for $A^+ = NH_4^+$. It is thought that A^+–layer interactions are maximised in the Φ_y structure due to the symmetry of the NH_4^+ cation [19]. Formation of LTMs with the Φ_x structure in the presence of sodium molybdate was only observed on reduction of the reaction pH to 5.0. Above this pH LDH reconstruction occurred preferentially. Analysis of the basal spacing and FTIR spectra of the resulting LDH confirmed the incorporation of CO_3^{2-} and not molybdate. The CO_3^{2-} anion is often incorporated into the LDH structure if no precautionary measures are taken due to its high abundance and strong interaction with the LDH interlayer [26]. Alternatively, the reaction time or molybdate concentration may not be sufficiently long or high for the incorporation of (polyoxo)molybdate species. Formation of terephthalate (TA^-) intercalated LDHs by rehydration of MMOs, for example, is thought to occur in two stages; reconstruction of an OH^-/CO_3^{2-} containing LDH followed by anion exchange with TA^-. The extent of anion exchange was dependent on the concentration of TA^- present [51]. Interestingly we have found that Anderson type materials can also be produced by this Green Chemistry method and note that they are also of catalytic interest.

Comparison of the LDH and LTM morphologies reveals similarities, both in terms of particle size and morphology, between the precursors and products of the MMO route. Levin et al. commented on the close structural relationship between the LDH and Φ_y LTM structure [23]. This suggests that the mechanism of LTM formation may be templated by the MMO particles in a similar idea to the 'memory effect' for LDH reconstruction. The mechanism of LDH reconstruction remains unclear. Initially it was

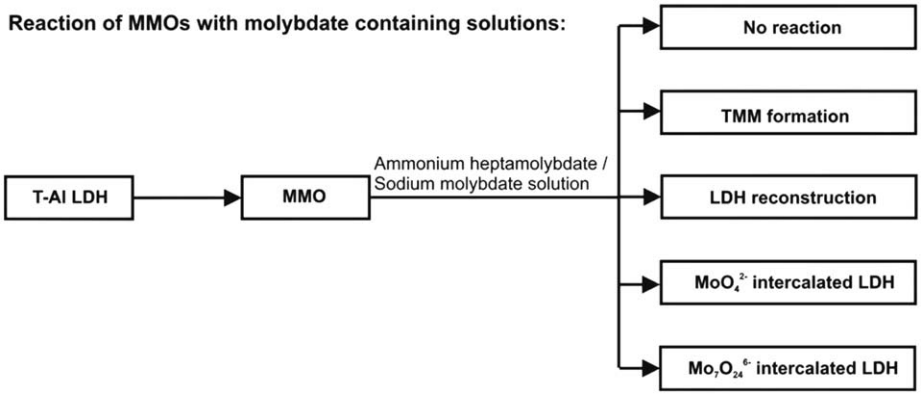

Fig. 11. Summary of potential outcomes on reaction of MMO with aqueous molybdate containing solution.

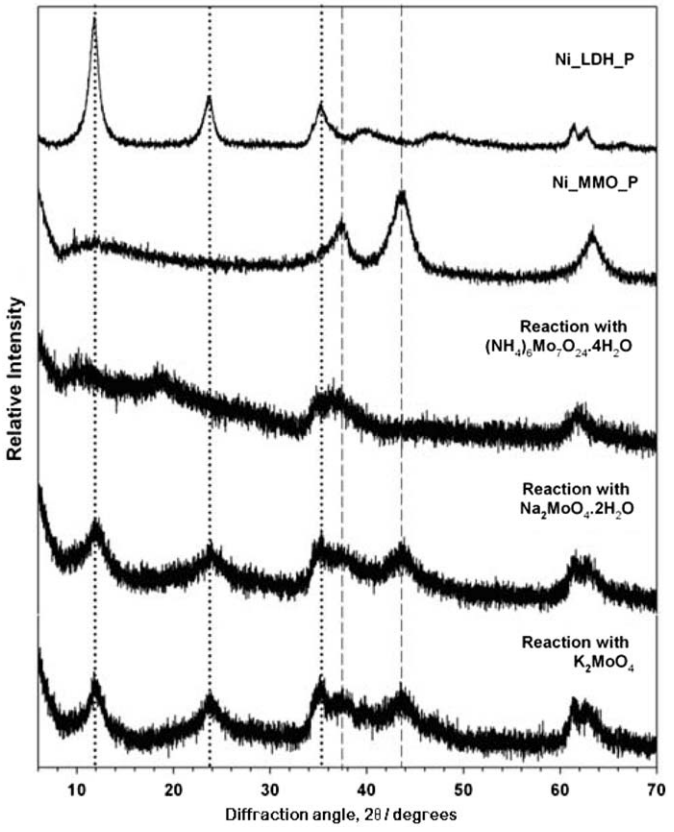

Fig. 12. Comparison of the PXRD patterns of the materials obtained following exposure of Ni_MMO_P phases to aqueous solutions containing ammonium heptamolybdate or sodium or potassium molybdate (Ni/Mo ≈ 1).

thought to occur topotactically [52] but recently convincing evidence for the occurrence of dissolution and recrystallisation during the rehydration process has been presented [53]. An *in situ* PXRD study showed that reconstruction of an Mg–Al MMO occurred rapidly with reflections corresponding to the LDH phase appearing 'almost instantaneously' on exposure to aqueous solution, even at room temperature [54]. In contrast, for the reaction of MgO with an amorphous alumina phase a delay was observed before the appearance of LDH reflections which was thought to be the consequence of an additional diffusion/mixing step required for LDH formation in that case [55]. It is possible that the two processes occur simultaneously to varying extents depending on the conditions studied. This might explain such conflicting arguments as that of 'no morphological change during reconstruction [56] with those who have shown growth of LDH crystallites on the surface of initial hydrotalcite plates [53].

The concept of simultaneous dissolution and recrystallisation with a templated crystal growth mechanism could explain not only the morphological resemblance of the LTM products derived from MMOs to their LDH precursors but also the differences in observed phase selectivity of reaction. As the Φ_x structure bears less of a resemblance to that of the precursor LDH than the Φ_y structure, its formation would require more significant rearrangement of the LDH structure. Lowering the reaction pH would favour increased dissolution of the precursor MMO phase, thus removing the presence of a templating phase and facilitating structural rearrangement through dissolution and recrystallisation.

Contrary to previous findings [23], compositional analyses of the LTM products derived from MMOs indicate little change in the quantity of Al present compared with that in the precursor LDHs. Levin et al. related the reactivity of a MMO towards LTM formation to the extent of Al dissolution during rehydration in order to explain why MMOs possessing the rocksalt structure, where the Al can remain in sites of octahedral coordination, are generally thought to be less reactive [23]. Segregation of Al during calcination and rehydration of LDHs have been reported by several studies [57]. A mechanism solely involving dissolution and recrystallisation, however, would not account for the significant presence of Al which we observe. This Al is possibly incorporated as an amorphous oxide phase or it could potentially be present in the LTM structure either as a charge balancing cation or occupying vacancies within the layer [16].

The possibility of finding an Al on a lattice site has previously been investigated by the attempted crystal structure refinement, based on Rietveld analysis, of the ammonium zinc molybdate structure. On refinement it was found that when a proportion of Zn lattice sites were replaced with Al, the fractional occupancy refined to zero indicating that this is not a likely possibility [23]. We applied ^{27}Al solid state NMR (not shown) to study the conversion of the Al^{3+} between octahedral and tetrahedral environments during calcination of the LDH precursors and on reaction of the resulting MMOs with ammonium heptamolybdate. On calcination we observed the expected conversion from chemical shifts of octahedral to tetrahedral coordination, corresponding to previously reported observations. Following reaction of the MMO with ammonium heptamolybdate a change in the NMR spectra is also observed, in this case with conversion from tetrahedral to octahedral coordination. Peaks due to both tetrahedral and octahedral Al^{3+} remain in the LTM

phases indicating that the Al is in more than one coordination environment.

We also studied the homogeneity of the LTM compositions by EDX analysis of a range of samples. This showed that there is little sample heterogeneity (areas with distinct chemical compositions) within the resolution limits of the electron microscope. This conclusion was supported by observation of the back scattered electron images which showed little phase contrast between particles. From these results we can conclude that if phase separation occurs during reaction of the MMO, for example if the Al is present as an amorphous alumina component, this must occur at a nanoscopic level.

Differences in the thermal properties of LTM products might be expected due to the presence of Al in those prepared from MMOs. Cu containing LTMs are found to have a slightly improved thermal stability compared to Zn containing TMMs and this may indicate a greater stability of the Φ_y structure with Cu.

5. Conclusions

Several possible reaction pathways exist for the reaction of MMOs derived from LDH precursors in aqueous molybdate containing solutions. MMOs of different compositions differ in their reactivity. For a given MMO the phase selectivity of the reaction is dependent on factors such as the nature of the countercation A^+, present in solution, the molybdate concentration and the reaction pH. Although LTMs prepared from MMOs appear isostructural to those obtained by precipitation synthesis they are found to have different compositions, morphologies and thermal properties. The preparation route of LDH precursors was also shown to influence both the crystallite size and thermal properties of the LTM products obtained.

Acknowledgments

The authors would like to acknowledge EPSRC and CSIC for funding. Morgane Presle and Aurélie Guenet, visiting students to the group, are thanked for their preliminary work in this area.

Appendix A. Supplementary material

Supplementary data associated with this article can be found in the online version at doi:10.1016/j.jssc.2009.10.011.

References

[1] M.M. Barsan, C.F. Thyrian, Catal. Today 81 (2003) 159–170.
[2] M. Honda, K. Tanaka, I. Watambe, DE Patent 2112938 19720127, 1972.
[3] M. Breysse, C. Geentet, P. Afanasiev, J. Blanchard, M. Vrinat, Catal. Today 130 (2008) 3–13.
[4] L. Barrio, J.M. Campos-Martin, M.P. de Frutos, J.L.G. Fierro, Ind. Eng. Chem. Res. 47 (2008) 8016–8024.
[5] J.M. Mitchell, N.S. Finney, J. Am. Chem. Soc. 123 (2001) 862–869.
[6] J.S. Chung, R. Miranda, C.O. Bennett, J. Catal. 114 (1988) 398–410.
[7] I.D. Ospina, L.A. Palacio, A. Echavarria, A. Simon, C. Saldarriaga, Micropor. Mesopor. Mater. 47 (2001) 303–309.
[8] D.Q. Chu, C.L. Pan, L.M. Duan, J.Q. Xu, L.M. Wang, J.H. Yu, T.G. Wang, Inorg. Chem. Commun. 5 (2002) 989–992.
[9] S. Lei, K. Tang, Q. Liu, Z. Fang, Q. Yang, H. Zheng, J. Mater. Sci. 41 (2006) 4737–4743.
[10] J.S. Xu, D.F. Xue, Y.C. Zhu, J. Phys. Chem. B 110 (2006) 17400–17405.
[11] R.Z. Ma, Z.P. Liu, K. Takada, N. Iyi, Y. Bando, T. Sasaki, J. Am. Chem. Soc. 129 (2007) 5257–5263.
[12] L.A. Palacio, A. Echavarria, D.A. Hoyos, C. Saldarriaga, Solid State Sci. 7 (2005) 1043–1048.
[13] A. Clearfield, A. Moini, P.R. Rudolf, Inorg. Chem. 24 (1985) 4606–4609.
[14] M. Jang, T.J.R. Weakley, K.M. Doxsee, Chem. Mater. 13 (2001) 519–525.
[15] D.Q. Chu, C.L. Pan, L.M. Duan, J.Q. Xu, L.M. Wang, J.H. Yu, T.G. Wang, Inorg. Chem. Commun. 5 (2002) 989–992.
[16] C.D. Wu, C.Z. Lu, X. Lin, S.F. Lu, H.H. Zhuang, J.S. Huang, J. Alloys Compd. 368 (2004) 342–348.
[17] H. Pezerat, I. Mantin, S. Kovacevi, Compt. Rend. 262 (1966) 95–98.
[18] L.A. Palacio, A. Echavarria, C. Saldarriaga, J. Inorg. Mater. 3 (2001) 367–371.
[19] D. Levin, S.L. Soled, J.Y. Ying, Inorg. Chem. 35 (1996) 4191–4197.
[20] S. Soled, D. Levin, S. Miseo, J. Ying, Stud. Surf. Sci. Catal. 118 (1998) 359–367.
[21] A. Moini, P.R. Rudolf, A. Clearfield, J.D. Jorgensen, Acta Crystallogr. C 42 (1986) 1667–1669.
[22] L.A. Palacio, A. Echavarria, C. Saldarriaga, Stud. Surf. Sci. Catal. 135 (2001) 2888.
[23] D. Levin, S.L. Soled, J.Y. Ying, Chem. Mater. 8 (1996) 836–843.
[24] A. Clearfield, M.J. Simms, R. Gopal, Inorg. Chem. 2 (1976) 335–338.
[25] H. Pezerat, Compt. Rend. 261 (1965) 5490.
[26] J. He, M. Wei, B. Li, Y. Kang, D.G. Evans, X. Duan, in: X. Duan, D.G. Evans (Eds.), Layered Double Hydroxides (Structure and Bonding), Springer, Berlin, 2006, pp. 89–119.
[27] A. de Roy, C. Forano, J.P. Besse, in: V. Rives (Ed.), Layered Double Hydroxides: Present and Future, Nova Science Publishers Inc., New York, 2001, pp. 1–40.
[28] M.T. Pope, Heteropoly and Isopoly Oxometalates, Springer, New York, 1983.
[29] T. Hibino, A. Tsunashima, Chem. Mater. 9 (1997) 2082–2089.
[30] M. Turco, G. Bagnasco, U. Costantino, F. Marmottini, T. Montaneri, G. Ramis, G. Busca, J. Catal. 228 (2004) 43–55.
[31] U. Costantino, F. Marmottini, M. Nocchetti, R. Vivani, Eur. J. Inorg. Chem. 10 (1998) 1439–1446.
[32] F. Kooli, C. Depege, A. Ennaqadi, A. de Roy, J.P. Besse, Clays Clay Miner. 45 (1997) 92–98.
[33] C.C. Allen, R.C. Burns, G.A. Lawrance, P. Turner, T.W. Hambley, Acta Crystallogr. C 52 (1997) 7–9.
[34] Z.P. Xu, G. Stevenson, C.Q. Lu, G.Q. Lu, J. Phys. Chem. B 110 (2006) 16923–16929.
[35] L.A. Lv, Y. Wang, M. Wei, H.J. Cheng, J. Hazard. Mater. 152 (2008) 1130–1137.
[36] M. Bouraada, M. Lafjah, M.S. Ouali, L.C. de Menorval, J. Hazard. Mater. 153 (2008) 911–918.
[37] S. Abello, F. Medina, D. Tichit, J. Perez-Ramirez, J.C. Groen, J.E. Sueiras, P. Salagre, Y. Cesteros, Chem.-A Eur. J. 11 (2005) 728–739.
[38] X.D. Lei, F.Z. Zhang, L. Yang, X.X. Guo, Y.Y. Tian, S.S. Fu, F. Li, D.G. Evans, X. Duan, A.I.Ch.E. J. 53 (2007) 932–940.
[39] P. Kovar, K. Melanova, V. Zima, L. Benes, P. Capkova, J. Colloid Interface Sci. 319 (2008) 19–24.
[40] C.A.S. Barbosa, A.M.D.C. Ferreira, V.R.L. Constantino, Eur. J. Inorg. Chem. (2005) 1577–1584.
[41] K. Chibwe, W. Jones, Chem. Mater. 1 (1989) 489–490.
[42] A.L. Maciuca, E. Dumitriu, F. Fajula, V. Hulea, Appl. Catal. A 338 (2008) 1–8.
[43] D. Carriazo, C. Martin, V. Rives, Catal. Today 162 (2007) 153–161.
[44] P. Atkins, C.L. Depege, C. Forano, M. Rene, US Patent 6124506, 2000.
[45] B.M. Choudary, S. Madhi, N.S. Chowdari, M.L. Kantam, B. Sreedhar, J. Am. Chem. Soc. 124 (2002) 14127–14136.
[46] E. Gardner, T.J. Pinnavaia, Appl. Catal. A 167 (1998) 65–74.
[47] D. Levin, J.Y. Ying, Stud. Surf. Sci. Catal. 110 (1997) 367–373.
[48] F. Kooli, V. Rives, M.A. Ulibarri, Inorg. Chem. 34 (1995) 5114–5121.
[49] P. Benito, I. Guinea, F.M. Labajos, V. Rives, J. Solid State Chem. 181 (2008) 987–996.
[50] J. Perez-Ramirez, G. Mul, F. Kapteijn, J.A. Moulijn, Mater. Res. Bull. 36 (2001) 1767–1775.
[51] E.L. Crepaldi, J. Tronto, L.P. Cardoso, J.B. Valim, Colloids Surf. A 211 (2002) 103–114.
[52] T. Sato, H. Fujita, T. Endo, M. Shimada, A. Tsunashima, React. Solids 5 (1988) 219–228.
[53] T.S. Stanimirova, G. Kirov, J. Mater. Sci. Lett. 20 (2001) 453–455.
[54] F. Millange, R.I. Walton, D. O'Hare, J. Mater. Chem. 10 (2000) 1713.
[55] S. Mitchell, T. Biswick, W. Jones, G. Williams, D. O'Hare, Green Chem. 9 (2007) 373–378.
[56] F. Delorme, A. Seron, M. Bizi, V. Jean-Prost, D. Martineau, J. Mater. Sci. 41 (2006) 4876–4882.
[57] T. Hibino, A. Tsunashima, Chem. Mater. 10 (1998) 4055–4061.